

## Portable microcontroller-based electrostimulation system for nerve conduction studies

Cossul, Sandra; Rettore Andreis, Felipe; Favretto, Mateus Andre; Antonio, Afranio de Castro; Marques, Jefferson Luiz Brum

*Published in:*  
IET Science, Measurement & Technology

*DOI (link to publication from Publisher):*  
[10.1049/iet-smt.2019.0174](https://doi.org/10.1049/iet-smt.2019.0174)

*Creative Commons License*  
CC BY 4.0

*Publication date:*  
2020

*Document Version*  
Accepted author manuscript, peer reviewed version

[Link to publication from Aalborg University](#)

### *Citation for published version (APA):*

Cossul, S., Rettore Andreis, F., Favretto, M. A., Antonio, A. D. C., & Marques, J. L. B. (2020). Portable microcontroller-based electrostimulation system for nerve conduction studies. *IET Science, Measurement & Technology*, 14(6), 695-703. <https://doi.org/10.1049/iet-smt.2019.0174>

### **General rights**

Copyright and moral rights for the publications made accessible in the public portal are retained by the authors and/or other copyright owners and it is a condition of accessing publications that users recognise and abide by the legal requirements associated with these rights.

- Users may download and print one copy of any publication from the public portal for the purpose of private study or research.
- You may not further distribute the material or use it for any profit-making activity or commercial gain
- You may freely distribute the URL identifying the publication in the public portal -

### **Take down policy**

If you believe that this document breaches copyright please contact us at [vbn@aub.aau.dk](mailto:vbn@aub.aau.dk) providing details, and we will remove access to the work immediately and investigate your claim.

# A portable microcontroller-based electrostimulation system for nerve conduction studies

Sandra Cossul<sup>1\*</sup>, Felipe Rettore Andreis<sup>1,2</sup>, Mateus André Favretto<sup>1</sup>, Afrânio de Castro Antonio Jr.<sup>1</sup>, Jefferson Luiz Brum Marques<sup>1</sup>

<sup>1</sup> Institute of Biomedical Engineering, Department of Electrical and Electronic Engineering, Federal University of Santa Catarina, Florianópolis-SC, Brazil

<sup>2</sup> Department of Health Science and Technology, Aalborg Universitet, Aalborg, Denmark

\*sandra.cossul@gmail.com

**Abstract:** Despite nerve conduction study (NCS) being an established procedure in the evaluation of neuromuscular disorders, its utility has been restrained by commercially available products or approaches presented in the literature that are either costly, physically large, dependent on specialized medical personnel to operate or targeted to specific conditions, evaluating only one or two nerves. Therefore, the objective of this work was to develop a point-of-care device for NCS that can be used to evaluate several nerves, yet is still portable, low-cost and easy to operate. The developed device is composed of three modules: (i) controller module and graphical user interface, responsible for system synchronization and configuration, data management, graphical visualization of the evoked action potential and stimulus voltage feedback (maximum error of 3.92%); (ii) stimulation module, which operates in a constant voltage mode and delivers a monophasic stimulus pulse with amplitudes between 0.84 V and 230 V, with a discrete increment of  $2.32 \pm 0.64$  V (mean  $\pm$  SD) and duration of 100  $\mu$ s or 200  $\mu$ s; and (iii) data acquisition module, based on the ADS1298 front-end that records the evoked action potentials after the stimulus, with a sample rate of 16 kHz or 32 kHz, 24-bit resolution and selectable voltage gain of 1 up to 12. Results demonstrated that the system could reliably deliver stimulation pulses through different loads (100  $\Omega$ , 1 k $\Omega$  and 10 k $\Omega$ ) and accurately record data through frequencies of 10 Hz up to 10 kHz. Additionally, NCS of the ulnar motor nerve in a sample of healthy individuals showed that the device could effectively activate a peripheral nerve and record compound action potentials within normal limits established by the literature.

## 1. Introduction

Nerve conduction study (NCS) is a technique that involves the activation of peripheral nerves through applying depolarizing electrical stimulus on the skin and measuring the response obtained, which can be either (i) sensory nerve action potential (SNAP), representing the sum of single nerve fibre action potentials, or (ii) compound muscle action potential (CMAP), arising from the activation of muscle fibres in a muscle supplied by the nerve being activated [1, 2].

Electrodiagnostic studies, including NCS and electromyography, are the gold standard for evaluating functions of peripheral nerves, neuromuscular junctions and muscles [3]. These tests are useful to study the continuity, excitability, anatomic course and the number of nerve fibres [4]. The NCS assessment of direct and indirect characteristics from the nerve response, such as amplitude, latency, duration, area and conduction velocity, provides information about nerves' functionality and allows for the localisation and characterisation of abnormalities [4, 5].

Nerve stimulation is accomplished by the application of a square-wave pulse to the skin over a target nerve, usually varying from 100 to 500  $\mu$ s in duration and 100 to 400 V in amplitude, assuming a tissue resistance of 10 k $\Omega$  [6]. According to Daube and Rubin (2012), a stimulus of 100 V and 100  $\mu$ s in duration is usually adequate to elicit a nerve response. However, for deep nerves, the stimulus may need to be as high as 300 V in intensity and 500  $\mu$ s in duration. Another requirement regarding the stimulators is that the

stimulus intensity must be gradually increased until the amplitude of the evoked response saturates, a phenomenon called "supramaximal" stimulus. The supramaximal stimulus is necessary for reliable measurements because it ensures activation of all nerve fibres [7]. As for the surface stimulation electrodes, typically they are made of silver plate probes 0.5 to 1.0 cm in diameter and 2 to 3 cm apart [6].

The equipment necessary to perform an NCS needs to include the following: (a) an electrical stimulator for proper nerve stimulation; (b) a recording module for acquiring the compound evoked potentials from the muscle, in the study of motor fibres, and from the nerve itself, in the case of sensory fibres; and (c) a controller to determine the stimulus intensity, synchronize the stimulus application with the recording and also configure the system (e.g., filters, amplifier gain). The device should further include a display (i.e., interface) for visually presenting the evoked nerve action potentials [6, 8].

The stimulator can be one of two types, either constant current or constant voltage. In the constant current type, the voltage changes according to the skin impedance to regulate the amount of current that reaches the nerve, maintaining the output at the desired adjustable current level. Meanwhile, in the constant voltage type, the current output varies inversely with the impedance of the electrode, skin and subcutaneous tissues [6, 8]. Additionally, the electrical stimulation devices must have control over the duration and intensity of the pulse for the application of a stimulus consistent with the configuration of the stimulus parameters, guaranteeing the safety of the subject [6]. Electrical stimulators should also be

isolated from the recording module and other equipment to reduce noise artefacts and increase safety, ensuring that the current flows only between the stimulation electrodes [4, 6].

The potentials assessed during an NCS range in amplitude from millivolts in motor studies (i.e., CMAPs varying from 1 to 15 mV) to microvolts in sensory studies (i.e., SNAPs varying from 1 to 50  $\mu$ V), with frequencies ranging from 2 Hz up to 10 kHz [2, 9, 10]. Typically, square-shaped surface electrodes with an average size of 1 x 1 cm are used for the recording [6]. A routine NCS uses a bipolar (i.e., differential) recording technique, whereby the active electrode signal is compared to that measured by the reference electrode and both are compared with a ground electrode [11]. For the action potential recording, the system needs to include a differential amplifier with an input impedance of at least 10 M $\Omega$ , low noise level and a high common-mode rejection ratio (i.e., 80 to 100 dB or higher) [6].

Electrodiagnostic systems such as Nicolet EDC (Natus Neuro, USA), Cadwell Sierra Summit (Cadwell Industries Inc., USA) and XLTEC NeuroMax (XLTEC, Canada) are available on the market for nerve conduction studies. Although those systems are complete solutions, they are costly, typically being above \$5000, and their utility is constrained by the physically large equipment design, therefore requiring that they are operated in a specific environment. Besides that imposition, trained specialists are necessary to handle such equipment, restricting even more the use of the exam and consequently, causing it to be employed only for confirmatory diagnosis [12, 13].

In recent years, automated NCS instruments have been becoming more popular as an innovation on the traditional systems, providing simpler solutions to be employed as point-of-care devices (POCD). As mentioned by [14], automated NCS enables primary care to make timely and objective decisions about patients with neuromuscular disorders, extending the clinical reach to a higher number of patients at earlier points in their illnesses. One typical example of such a device is the DPNCheck [15, 16], which is a POCD for diagnosis of diabetic peripheral neuropathy however, evaluates only the sural nerve. Another handheld nerve conduction device was proposed by [17] as a diagnostic utility for carpal tunnel syndrome; however, it tests only two nerves (i.e., the median and ulnar nerves). Besides that devices, other nerve stimulators have been proposed, including neural interfaces [18], functional electrical stimulation [19], and neuromodulation [20].

Despite the availability of traditional NCS equipment and, more recently, of automated NCS devices, the firsts ones were designed to be handled by specialists, in support of a wide variety of testing modalities. By contrast, the newer approaches provide convenient options but are targeted to specific conditions and examine only one or two nerves. NCS devices designed to perform nerve conduction testing at several nerves, yet portable, easily operated, and low-cost options are still lacking.

Therefore, the objective of this work is to develop a point-of-care device for nerve conduction studies that includes an electrical stimulator, a recording module and a graphical user interface. The main contributions of this work are the following: (a) a novel stimulator and recording circuit design; (b) stimulation parameters digitally controlled with feedback, increasing the device safety; (c) nerve conduction

testing of several nerves, being necessary only to change the electrode configuration and (d) portability and ease of operation, consequently making the device easy to transport and quickly employ in a clinical facility.

## 2. System Overview and Methods

### 2.1 Electrostimulation Device

The developed system is composed of three modules: (i) controller module (CM), responsible for the system synchronization, data management and graphical visualization; (ii) stimulation module (SM), which generates the electrical stimulus; and (iii) the data acquisition module (DAM), which registers the evoked potentials after the stimulus.

The CM includes the Teensy 3.2 (PJRC, USA) microcontroller ( $\mu$ C) and the graphical user interface (GUI), which configures and synchronises the system, and the module is also responsible for the data management from the DAM and transmission via USB to the GUI for visualisation and further processing. This module communicates via I2C (inter-integrated circuit) with the SM and via SPI (serial peripheral interface) with the DAM.

The system is electrically isolated within the modules to improve safety and reduce stimulus artefacts. Thus, stimulus current flows only in the stimulus electrodes, avoiding conductive paths that could lead to stimulus artefacts, recording amplifier saturation or even stimulation at unintended sites [6]. The device's schematic is shown in Fig.1.

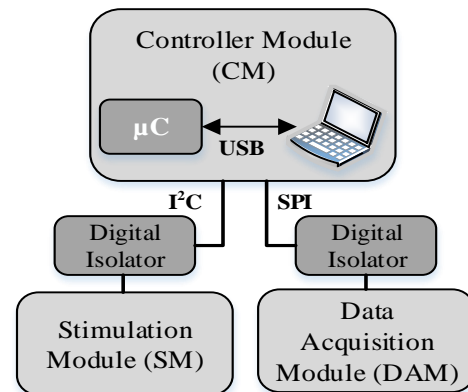


**Fig. 1** Schematic of the device. The three modules: stimulation (SM), controller (CM) and data acquisition (DAM) are isolated in the communication (i.e., I<sup>2</sup>C digital isolator between the CM and the SM and SPI digital isolator between the CM and the DAM). The CM communicates via USB with the graphical user interface. More details of the modules are described below.

**2.1.1 Stimulation Module:** The developed stimulator operates in a constant voltage mode and generates monophasic square wave pulses, with continuously adjusted voltage amplitude and pre-configured pulse parameters (i.e., duration and stimulation rate). This module can be divided into four main operational blocks: DC/DC converter, adjustable voltage regulator circuit, pulse generator and half-bridge circuit. The high voltage (HV) generated in the DC/DC

converter is regulated from zero to maximum (0 – HV) and then transferred to the half-bridge circuit which, in turn is switched on when a pulse is applied in its input generating an output stimulus pulse with amplitude equal to the regulated voltage. The SM is digitally controlled; therefore, the CM sends configuration commands that set the pulse parameters, trigger the pulse generator and regulate the digital potentiometer.

The SM is powered by a 12 V medical power supply, model SM12-12-E (CUI Inc., USA), which is certified according to the IEC 60601-1 safety approvals. This voltage is scaled down to 5V with a voltage regulator (LM78L05, Texas Instruments, USA) and elevated to a fixed voltage of 290 V with a DC/DC converter. The DC/DC converter is a high voltage boost module with a voltage input of 10 to 32 V (5 A max.), an adjustable voltage output of 45 V to 390 V (200 mA), and an operating frequency of 75 kHz. The adjustable voltage regulator circuit, the half-bridge circuit (IR2111, International Rectifier, USA) and the level shifter circuit are supplied by 12 V, while both the  $\mu$ C for pulse generation and the digital potentiometer (TPL0401, Texas Instruments Inc., USA) are supplied by 5 V.

Both being supplied by 5V, the I<sup>2</sup>C digital isolator ISO1541 (Texas Instruments Inc., USA) was selected for communication and the isolation amplifier AMC1100 (Texas Instruments Inc., USA) for voltage measurement. The block diagram of the SM is shown in Fig. 2. Even though the DC/DC converter can be regulated, it was necessary to develop a fine voltage regulator to obtain more precision in the voltage setting. Thus, the adjustable voltage regulator circuit sets the pulse amplitude and therefore controls the stimulus level. The circuit can be divided into two operation steps: voltage comparator and driver, as detailed in Fig. 3. In the first step, an operational amplifier (LM358, Texas Instruments Inc., USA) was used as a comparator. A

reference voltage was applied to the inverting input, which was obtained from a voltage divider (R3 and R4) controlled by the adjustment of a 10 k $\Omega$  digital potentiometer (TPL0401, Texas Instruments Inc., USA). The regulated output voltage ( $V_{REG}$ ), or feedback voltage, was connected to the non-inverting input, which was scaled down to the op-amp operating voltage range by a voltage divider (R7 and R8). In the second step, the op-amp output was connected to a power MOSFET transistor (IRF840, Vishay Siliconix, USA), which was connected to a second MOSFET transistor (IRF840, Vishay Siliconix, USA) that performs the charge control of the capacitor (C1). The capacitor discharge occurs by the same resistors (R7 and R8) used for the feedback voltage divider. For transistor gate protection, a 12 V Zener diode was used.

The reference voltage ( $V_{REF}$ ) obtained from the digital potentiometer adjustment controls the switching of the transistors, which in turn controls the capacitor (C1) charge, resulting in a regulated output voltage ( $V_{REG}$ ). Therefore,  $V_{REG}$  is continuously compared with  $V_{REF}$  and can be adjusted over the range of approximately 0 V to HV (i.e., 230 V in this circuit).

For correct circuit operation, the two inputs of the comparator must have similar voltage ranges, a factor that depends on the combination of the resistors in the input voltage divider (R3 and R4) and in the feedback voltage divider (R7 and R8). For example, considering a circuit setting of 0 to 250 V and  $V_{CC} = +12$  V, the input divider resistors could be combined with 10 k $\Omega$  and 15.6 k $\Omega$  and the feedback resistors combined as 2.7 M $\Omega$  and 47 k $\Omega$ , resulting in output voltages of 4.68 V and 4.27 V, respectively. These values may vary depending on the operating range of the voltage regulator.

To conclude the description of the stimulation system's blocks, the half-bridge circuit was implemented with two

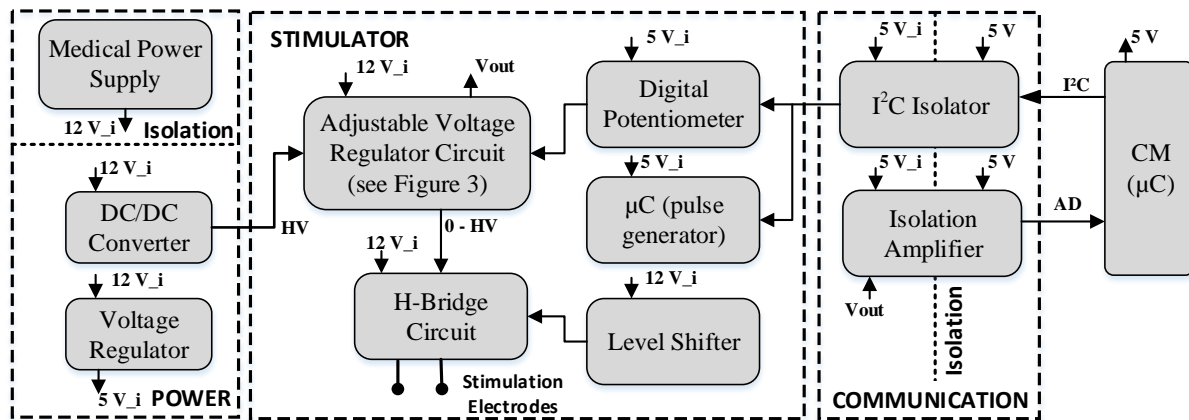


**Fig. 2** Block diagram of the stimulation module (SM). The SM is powered by 12 V isolated (12 V<sub>i</sub>) with a medical power supply and down regulated to 5 V (5 V<sub>i</sub>). The DC/DC boost converter elevates the 12 V to a high voltage (HV) that is fine regulated from 0 to HV with an adjustable voltage regulator circuit (see details in fig. 3) that, in turn, is controlled by a digital potentiometer from the user interface. This regulated voltage is transferred to a half-bridge circuit that outputs the stimulus pulse to the stimulation electrodes after switched on by a pulse generated in the microcontroller ( $\mu$ C), also controlled from the user interface. The level shifter is used to translate the voltage from the  $\mu$ C to the same voltage domain of the h-bridge circuit. Before the stimulus application, the regulated voltage ( $V_{out}$ ) is measured by an isolation amplifier and read by the  $\mu$ C's analogue pins, providing feedback of the stimulus amplitude. The communication with the controller module (CM) is via isolated i<sup>2</sup>C.

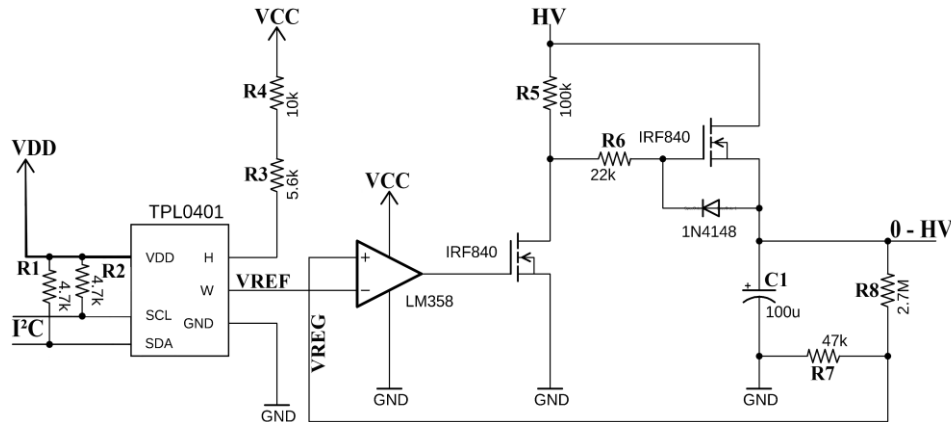


**Fig. 3** Adjustable voltage regulator circuit including the voltage comparator (op-amp LM358) and driver circuit. The reference voltage ( $V_{REF}$ ) obtained from the digital potentiometer (TPL0401) adjustment controls the switching of the transistors (IRF840), which in turn, controls the capacitor ( $C1$ ) charge resulting in a regulated output voltage ( $V_{REG}$ ), from 0 to HV. In this circuit,  $VCC = 12\text{ V}$  isolated,  $VDD = 5\text{ V}$  isolated and  $HV \approx 230\text{ V}$ . The digital potentiometer communicates via I<sup>2</sup>C with the controller module; R1 and R2 are pull-up resistors.

MOSFETs transistors IRF840 (Vishay Siliconix, USA) and IR2111 (International Rectifier, USA), which is designed for half-bridge applications.

The half-bridge circuit outputs a monophasic stimulation pulse after a switching pulse (or trigger pulse) is applied in its input. The trigger pulse is generated by a second microcontroller (Arduino Nano) inside the SM. The stimulus level depends on the value of  $V_{REG}$  and the pulse period is the same as the trigger pulse period. The pulse parameters (amplitude, period and number of sequential pulses) are user-controlled, with typical period values of 100  $\mu\text{s}$  and 200  $\mu\text{s}$ .

**2.1.2 Data Acquisition Module:** The DAM module records compound evoked potentials from the muscle in the study of motor fibres (i.e., CMAP) and from the nerve itself in the study of sensory fibres (i.e., SNAP); these potentials are generated after the application of an electrical stimulus from the SM.

This module was developed based on the ADS1298 (Texas Instruments Inc., USA), which is an analogue front-end for biopotential measurements. This component is an integrated solution for medical instrumentation systems that operates at low power (0.75 mW/channel) and low input noise (4  $\mu\text{V}_{PP}$ , 150 Hz BW, G=6) and has common-mode rejection ratio of 115 dB, programmable gain, high-resolution analogue-to-digital (A/D) converters (24 bits) and high data rates (250 Hz to 32 kHz).

Anti-aliasing filters are placed at the input channels of the ADS1298 to attenuate high frequencies. The filters are passive second order, with a cut-off frequency of approximately 67.5 kHz. The recorded data is sent to the CM via an SPI digital isolator (ISO7141, Texas Instruments, USA). The module is battery-powered (3.7 V) with voltage regulators that generate amplitudes of -2.5 V (LP5907, Texas Instruments, USA), +2.5 V (TPS723, Texas Instruments, USA) and +3.3 V (LP5907, Texas Instruments, USA). The battery is recharged using the IC TP4056 (Nanjing Top Power, China), which is a micro USB module battery charger (5 V, 1 A). The module's block diagram is represented in Fig.4.

### 2.1.3 Controller Module and Graphical User Interface (CM and GUI):

The CM includes the development board Teensy 3.2 (PJRC, USA) microcontroller and the GUI, designed with Microsoft Visual Studio C# 2017. The Teensy 3.2 is a USB-based microcontroller development system, compatible with Arduino software and libraries with the following specifications: 32 bit Arm Cortex-M4 (MK20DX256), 72 MHz processor; 256 KB of flash memory; 64 KB of RAM memory; 34 digital I/O pins (3.3 V, 5 V tolerance); 21 analogue pins; and UART, I<sup>2</sup>C and SPI.

The GUI configures the system's modules and presents the evoked action potentials after the electrical stimulus. Firstly, the USB communication is initialised, then, the GUI sends configuration parameters to the DAM setting the device for data capture, according to the selected stimulation protocol. Secondly, the GUI sends commands to the SM to regulate the voltage that will generate the amplitude of the stimulus pulse. The regulated voltage is continuously monitored and presented in real-time in the GUI. The stimulus intensity and its single application can be controlled automatically by selecting a stimulation protocol or manually by the user through the increment, decrement and pulse buttons.

The implemented stimulation protocols are called supramaximal, average and manual. In the supramaximal protocol, successive stimuli are applied with automatic voltage increases until the amplitude of the response action potential remains similar to the previous ones. The second of these protocols implement the averaging technique, which adds and scales synchronised signal responses to improve the signal-to-noise ratio [7, 8, 21]. Thus, many successive supramaximal stimuli are delivered, so that the signal presented at the end is the average of all action potentials, obtained individually after each stimulus. Finally, in the manually configured stimulation protocol, the user can configure the voltage amplitude, voltage gain (1 to 12), data acquisition rate (16 kHz or 32 kHz), period of the stimulus pulse (100  $\mu\text{s}$  or 200  $\mu\text{s}$ ) and the number and rate of stimulus delivery.



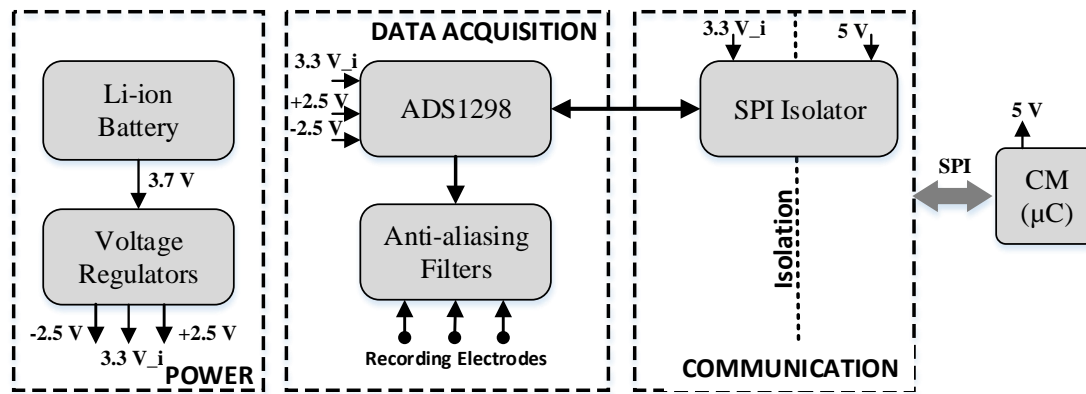


**Fig. 4** Block diagram of the data acquisition module (DAM). The DAM is powered by a rechargeable 3.7 V Li-ion battery and regulated to -2.5 V, +2.5 V and 3.3 V<sub>i</sub>, necessary to supply the ADS1298. ADS1298 is a front-end for biopotential measurements. Anti-aliasing passive filters are used in the input channels. Three surface electrodes are used for signal recording (i.e., active, reference and ground). The communication with the controller module (CM) is via isolated SPI. The CM is responsible for the ADS1298 configuration and also for the commands to start and stop data acquisition.

The GUI synchronises the modules; therefore, the signal recording initiates approximately 10 ms before the electrical stimulus is applied. The system registers the signal for 100 ms and, after passing the signal through digital filters, illustrates it in the interface's graph. Additionally, the GUI allows for saving the acquired data for further offline analysis.

Together with the GUI, the microcontroller receives the user commands and configures the modules and integrated circuits. The  $\mu\text{C}$  first initialises the communication protocols (SPI and I<sup>2</sup>C) and pre-configures the ADS1298, then receives the user-selected settings (i.e., digital potentiometer value, stimulation protocol, voltage gain and data acquisition rate) and configures the integrated circuits accordingly. After that process, the data is acquired and sent in packets to the GUI. Also, the  $\mu\text{C}$  continuously reads the A/D pins to acquire the regulated voltage of the system, sending the value to be shown in the GUI as a feedback voltage. The flowchart detailing the microcontroller's firmware is shown in appendices as Fig. 14.

## 2.2 Device Test Methodology

**2.2.1 Stimulation Module:** The SM was evaluated with tests related to the stimulus waveform and the voltage output control. In the first test, the stimulus pulse amplitude and width were measured. The voltage was increased from 0 to 200 V by steps of 10 V. In each step, the voltage was read by the GUI (10 samples for 30 s), and the output waveform was measured by an oscilloscope (Tektronix, model DPO 2012B, USA). This procedure was repeated with loads of 100  $\Omega$ , 1 k $\Omega$  and 10 k $\Omega$ . The protocol was performed for pulse widths of 100  $\mu\text{s}$  and 200  $\mu\text{s}$ .

In the second test, the output control of the electrical stimulus was evaluated according to the international standard IEC 60601-2-40, which applies to the basic safety and essential performance of electromyographs and evoked response equipment. One requirement of the standard establishes that an output control of the electrical stimulus must be incorporated in the device; thus, the output should vary from the minimum to the maximum voltage, in continuous or discrete mode, with maximum increments of

1mA or 5V. Furthermore, in its minimum position, the stimulus output voltage should not exceed 2% of the maximum available voltage.

A test was performed to assess this requirement. Initially, the device was set to its minimum position; after this, a charge of 1 k $\Omega$  was kept fixed at the output, and the voltage was increased in unit steps up to the maximum voltage range of the stimulator, totalling 128 steps. The voltage was read and presented in the GUI.

**2.2.2 Data Acquisition Module:** The DAM was tested through the application of sine waves with known frequencies in the input channel. These were compared with the acquired signal after fast Fourier transform.

For generating analogue input sine wave signals, a signal generator (B&K Precision, model 4005 DS, USA) was used. To verify the maximum signal gain, sine waves with a peak amplitude of 160 mV were applied in the input channel. The sine wave frequencies were variously 10 Hz, 20 Hz, 100 Hz, 500 Hz and finally 1 kHz to 10 kHz in intervals of 1 kHz. The signal was then recorded for 1 s, with a gain equal to 12 and a sampling frequency of 32 kHz. Afterwards, an offline analysis was performed in MATLAB (Mathworks Inc., USA).

## 2.3 Nerve Conduction Study in Healthy Individuals

To verify the correct functioning of the prototype system, a nerve conduction study of the ulnar motor nerve was performed with a group of 25 healthy volunteers aged  $27.8 \pm 7.67$  years (mean  $\pm$  SD). The study received prior approval from the Research Ethics Committee of the Federal University of Santa Catarina (Protocol number: 2.390.994), and informed consent was obtained from each subject.

The NCS was performed observing standard techniques of supramaximal percutaneous nerve stimulation and surface recording. The stimulation protocol was manual and the stimulus intensity was gradually increased by increments of approximately 10 V each to a level 10 % higher than the point where the resultant waveform did not increase in amplitude or area. The same examiner, using an orthodromic technique [6], performed all the tests. For the stimulation, surface

electrodes with felt pads soaked in saline solution were used. CMAPs were registered with single-use surface electrodes, with the recording electrode placed above the motor point. Stimulus duration was set to 100  $\mu$ s, and the sampling frequency was set to 32 kHz. The low- and high-frequency digital filter settings were 3 Hz and 10 kHz, respectively, and a notch filter was used to attenuate the 60 Hz interference. Ambient temperature was maintained above 25 °C to reduce measurement variability.

The ulnar nerve was stimulated at the wrist (S1) and below the elbow (S2). Recording electrodes were placed above the abductor digiti minimi (ADM) muscle (active) and distally over the fifth digit (reference). A ground bracelet electrode was placed between the stimulus and recording electrodes (GND). The examination was performed with the subjects seated, their knees and hips flexed at 90°, arm relaxed over a table, abducted at 60-90° and flexed at 90° (see protocol illustration at Fig. 5).

Data was extracted from the ulnar CMAPs, including distal and proximal latencies, amplitude, duration, area and nerve conduction velocity. For all parameters, descriptive statistics were calculated. The results were presented as mean $\pm$ 2\*standard deviation and as percentiles (5% - 95%).

The results obtained were compared with the results of normative studies found in the literature [6, 9, 10, 22, 23] that were developed under similar protocols. Unilateral one-sample *t*-tests were performed with alternative hypotheses established according to the available reference value (i.e., reference value from another study > X or < X, where X represents the mean value from a parameter obtained with the sample of healthy individuals of this study). Also, a paired *t*-test was used to compare the area and the amplitude between distal and proximal stimulus points. For the tests, a statistical significance of 5% was established

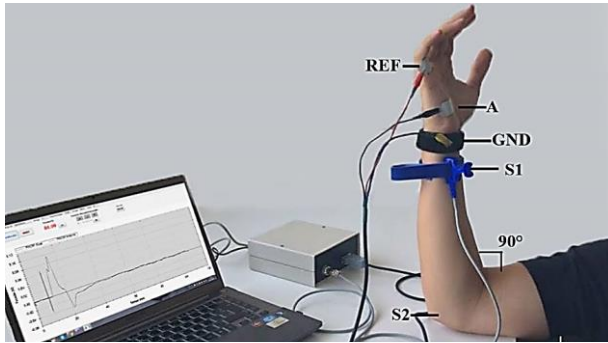


**Fig. 5** Protocol illustration of the ulnar motor nerve conduction study, stimulated at the wrist (S1 - distal point) and below the elbow (S2 - proximal point). Recording electrodes were placed above the abductor digiti minimi muscle (A - active), distally over the fifth digit (REF - reference) and between the stimulus and recording points (GND - ground).

### 3. Results

#### 3.1 Prototype Device and Tests

The circuit boards of the SM and DAM are represented in Fig. 6(a) and Fig. 6(b), respectively. The circuit boards and other components (battery, DC/DC converter module and connectors) were placed inside a plastic box with dimensions of 15 x 15 x 6 cm (see Fig. 7).

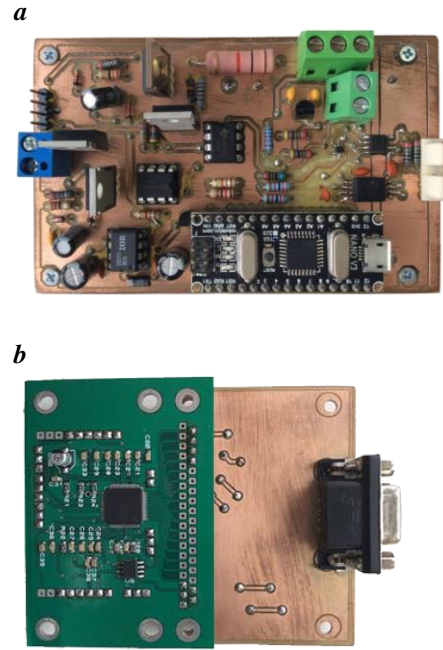


**Fig. 6** System circuit boards. (a) Stimulation module (b) Data acquisition module.



**Fig. 7** The final prototype of the developed device. (a) Recording cable. (b) Stimulation cable.

The GUI (see Fig. 8) is the system software control, allowing the user to set the protocol and stimulation parameters, control the stimulus intensity (Fig. 8(c)) providing feedback visualization (Fig. 8(b)), manually apply a stimulus (Fig. 8(d)) and also visualize the nerve action potential signal after data acquisition (Fig 8(a)) and save it for further analysis.

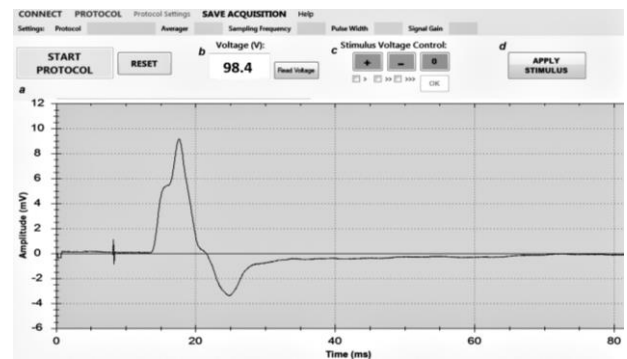


**Fig. 8** System's graphical user interface. (a) Illustrative graph of the compound muscle action potential recording. (b) Applied voltage level feedback. (c) Manual adjustment of the stimulus intensity. (d) Manual control of stimulus application.

The stimulus waveforms with pulse widths of 100  $\mu$ s and 200  $\mu$ s, from the first test of the SM, are shown in Fig. 9. The stimulus amplitude varied from 0.84 to 210 V. When compared to the voltage values measured by the system and presented in the GUI, the mean variation was 2.82%, and the maximum variation was 3.92%.

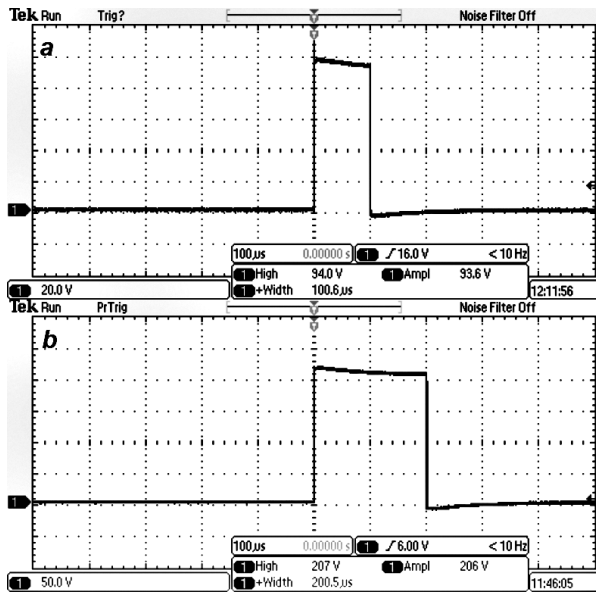


**Fig. 9** Measured stimulation waveforms (100  $\mu$ s/division). (a) A (Amplitude) = 93.6 V (20 V/div). (b) A = 206 V (50 V/div).

In the second test, concerning the voltage unit increment, the stimulus amplitude was 0.84 V at the minimum position and 226 V at the maximum position. The voltage increments had a variation of  $2.32 \text{ V} \pm 0.64 \text{ V}$ , with a maximum unit increment of 4 V, as represented in Fig. 10.

The DAM module was tested with an application of sine wave signals with known frequencies in the input channel.

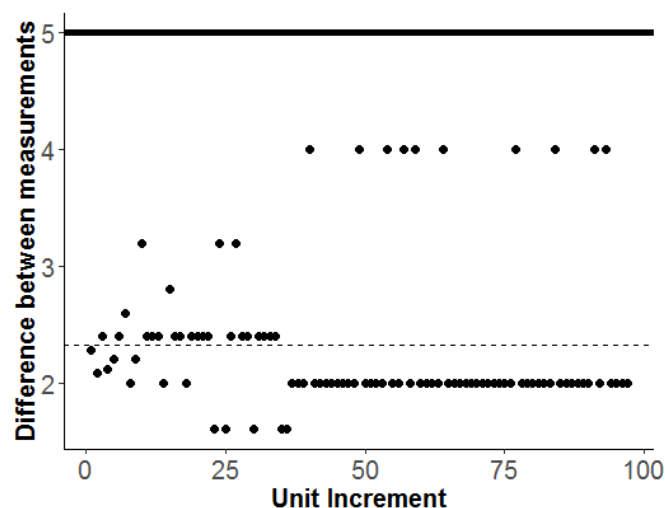


**Fig. 10** Unit increment versus the voltage difference between successive increments. The limit of 5 V by unit increment established by the norm is represented by the bold line and the voltage mean variation is represented by the dashed line.

The amplitude spectrum of the acquired signals is shown in Fig.11. The signals have an amplitude of approximately 2 V (160 mV  $\times$  gain 12 = 1.92 V). It was observed that for all acquired sine waves, the signal has its highest amplitude at the same frequency as the signal applied in the input. However, a decrease in the amplitude can be observed as the signal input frequency increases; this can be explained due to low-pass digital decimation filters presented in the ADS1298 (Texas Instruments Inc., USA) with a cut-off frequency of 8,384 Hz, which is computed as  $0.262 \times$  sampling frequency (in this case,  $0.262 \times 32 \text{ kHz}$ ).

### 3.2 Nerve Conduction Study in Healthy Individuals

The acquired signals were processed offline in MATLAB (MathWorks Inc., USA) to detect characteristic points (e.g., stimulus artefacts, maximum amplitude, and beginning of the action potential). The following parameters were then analysed from the ulnar CMAP, as illustrated in Fig. 12: latency, measured from the stimulus artefact to the onset of response (marker 1 to 2); amplitude, from baseline to negative peak; duration, from the onset to the first baseline crossing (marker 2 to 4); and area, considered under the duration interval. In addition, motor nerve conduction velocity was calculated by the distance between stimulation sites divided by the difference between proximal and distal latencies.

The results from the ulnar motor nerve conduction studies are shown in Fig. 13, and the reference data ranges are presented in Table 1. The  $t$ -tests performed with values of ulnar motor nerve conduction studies from the healthy group rejected the null hypothesis ( $p < 0.05$ ); that is, all parameters' values were within normal limits. According to the paired  $t$ -test, the distal amplitude and area values were significantly higher than proximal values ( $p < 0.05$ ). From the distal to the proximal stimulation site, the amplitude decreased by an average of 8.69%, while area decreased by an average of 6.25%.



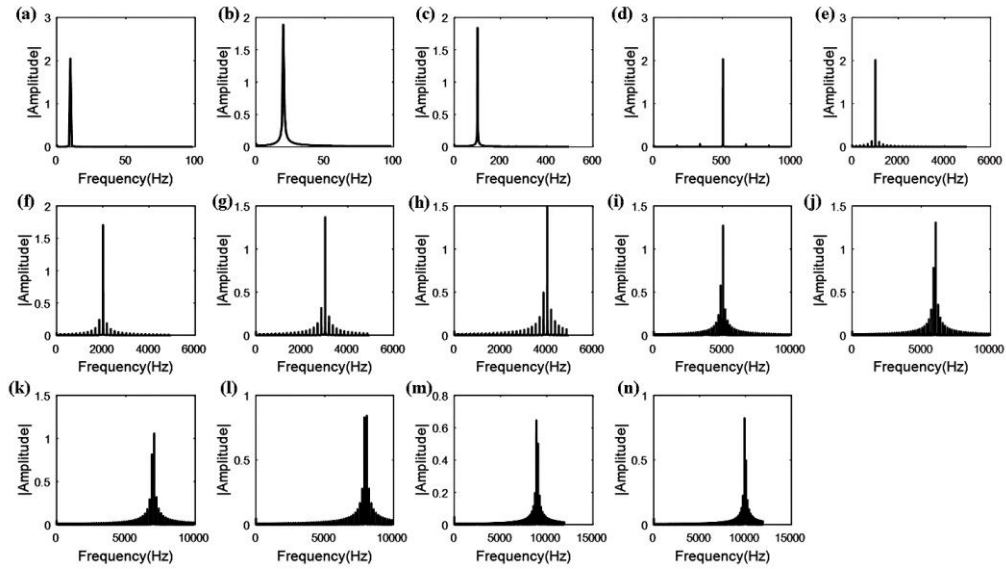


**Fig. 11** The amplitude spectrum of the acquired signals with an amplitude of 160 mV, sampling frequency of 32 kHz and gain 12. (a) 10 Hz. (b) 20 Hz. (c) 100 Hz. (d) 500 Hz. (e) 1 kHz. (f) 2 kHz. (g) 3 kHz. (h) 4 kHz. (i) 5 kHz. (j) 6 kHz. (k) 7 kHz. (l) 8 kHz. (m) 9 kHz. (n) 10 kHz.

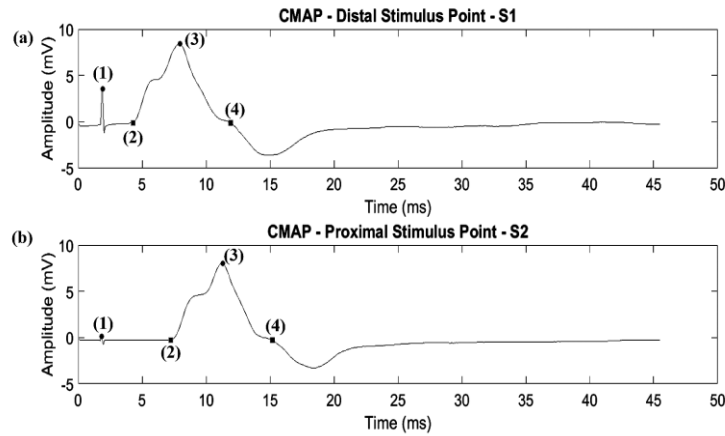


**Fig. 12** Compound muscle action potentials of ulnar nerve elicited from (a) distal and (b) proximal stimulus point. (1) stimulus artefact. (2) onset of response. (3) negative peak. (4) baseline crossing.

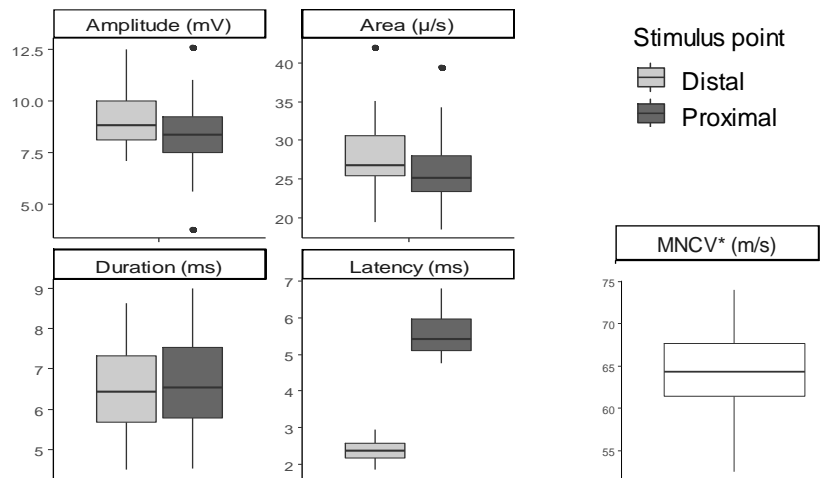


**Fig. 13** Nerve conduction measurements for ulnar motor nerve conduction study. \*MNCV = Motor Nerve Conduction Velocity.

**Table 1** References range defined as mean  $\pm$  2 SD and with the 5<sup>th</sup> and 95<sup>th</sup> percentile.

	Distal Stimulus Point				MNCV* (m/s)
	Amplitude (mV)	Latency (ms)	Duration (ms)	Area ( $\mu$ V. s)	
Mean $\pm$ 2 SD	6.3 – 11.9	1.8 – 3.0	4.2 – 8.6	18.0 – 37.2	50.7 – 76.3
Percentiles (5% - 95%)	7.2 – 11.4	2.0 – 2.8	4.5 – 8.2	21.4 – 34.5	55.4 – 71.7
	Proximal Stimulus Point				MNCV* (m/s)
	Amplitude (mV)	Latency (ms)	Duration (ms)	Area ( $\mu$ V. s)	
Mean $\pm$ 2 SD	4.7 – 11.9	4.4 – 6.8	4.4 – 8.8	16.6 – 35.0	
Percentiles (5% - 95%)	5.6 – 10.9	4.8 – 6.6	4.9 – 8.0	19.6 – 33.7	

\*MNCV – Motor Nerve Conduction Velocity

#### 4. Discussion

This work presented the development of a portable and digitally controlled electrical stimulator aimed at applications in nerve conduction studies. The system includes three integrated modules: control and user interface, stimulation and data acquisition.

The electrostimulation device operates in a constant voltage mode and delivers a monophasic stimulus pulse. The default operable characteristics of the device are the following: one stimulus channel; pulse duration configurable to 100  $\mu$ s or 200  $\mu$ s; output voltage up to 230 V; frequency of 1 Hz; and one recording channel with 24-bit resolution, 32 kHz sample rate, selectable gain of 1, 2, 4, 6, 8 or 12, common-mode rejection ratio of 115 dB and power supply rejection ratio of 90 dB. The system communicates via USB. The performance of the system was evaluated with regard to stimulus generation and data acquisition and validated with tests of NCS in a group of healthy subjects. The tests of the SM demonstrated an adequate generation of the stimulus pulses, delivering a stimulus in conformity with the configured duration and amplitude. Additionally, with regard to the insulation of the equipment, the modules were isolated from one another, with separate power supplies for the DAM (battery) and the SM (isolated source for medical equipment).

In the tests to compare the voltage reading by the GUI with the actual pulse amplitude value, the variation increased as the voltage increased; this may be due to the load control circuit, which exhibits a higher oscillation at higher voltages. Nonetheless, the average variation was 2.82%, and the maximum variation did not exceed 4.0%. This value is considered low and can occur due to the intrinsic non-ideality of the components used (e.g., op-amps, transistors, resistors and capacitors) or to the error in the voltage measurement circuit itself (CI AMC1100), which presents a gain error of 0.05% and a nonlinearity error of  $\pm$  0.023%.

In the tests to evaluate the voltage increase by unit increment, the voltage measured in the maximum increment was 226 V while in the minimum increment (or position) the voltage was 0.84 V. This is in accordance with the standard IEC 60601-2-40 (i.e., the voltage in the minimum position should not exceed 2 % of the maximum voltage). Also, it is possible to verify that the output voltage in each discrete increment did not exceed the limit of 5 V established by the norm, presenting values of  $2.32 \pm 0.64$  V (mean  $\pm$  SD) by increments. Therefore, the equipment complied with these standard items and was demonstrated to be safe with respect to the voltage output control.

About the DAM, the development of the circuit was facilitated due to the use of the front-end ADS1298, which was explicitly designed for biopotential measurements using A/D converters with high-resolution (24 bits), built-in amplifiers; the device also operates at a sample rate as high as 32 kHz. Although this integrated circuit has eight channels, only one channel was incorporated into the system. Future versions can include multiple recording sites, making fairly straightforward use of the other channels of the acquisition circuit [24].

The tests to evaluate the data acquisition module indicated the correct reading of the sine waves in different frequencies. Therefore, this module operated adequately without loss of data, when configured to a sampling frequency of 32 kHz and a gain of 12. A decrease of the signal's magnitude at higher frequencies is observed due to the cut-off frequency of the digital filters that occurs at approximately 8 kHz. The system was developed specifically for nerve conduction studies in which surface electrodes are used for recording. Consequently, the system frequency response was adequate, since the CMAP contains primarily components of low frequency (below 1000 Hz), whereas the SNAP has a broader range of frequency components (below 3000 Hz). An electrodiagnostic test could include intramuscular electromyography; in this case, the recording system has to respond to higher frequency components (up to 10 kHz) relative to fibrillation potentials, motor unit potentials (MUP) and single fibre MUPs [10, 25].

The graphical interface developed for the electrical stimulation system showed a correct functioning in the reading, display and storage of the signals, as well as in the configuration and communication with the hardware (i.e., the acquisition module). In the same way, it proved to be robust in the control and application of the pulses, allowing the increase and decrease of the voltage in a fast and continuous way. Additionally, the GUI was able to correctly control the synchronisation between the beginning of the recording of the nerve action potential and the application of the stimulus. The interface also allows the user to change the stimulus settings, such as the duration and frequency, thus making it possible to use the developed device in other applications (e.g., muscle stimulation).

The ulnar motor NCS performed on a sample of healthy individuals showed that the device could effectively activate a peripheral nerve and record compound action potentials. The NCS parameters (i.e., amplitude, latency, duration, area and motor nerve conduction velocity) derived from our

sample were consistent with reference data ranges presented in similar works [6, 9, 10, 22, 23]. For example, considering the ulnar motor nerve, a distal amplitude higher than or equal to 6 mV [10] or a distal latency below 3.7 ms [23] is within normal limits; in our results, the mean distal amplitude was 9.1 mV, while the mean distal latency was 1.7 ms. Also, according to [7], a reasonable reduction in area and amplitude is less than 20%, with stimulation between the wrist or ankle and elbow or knee. So, the observed mean reductions of 8.69% and 6.25% for amplitude and area, respectively, were within the expected decrease.

The following are the contributions of the device developed in this work: (a) portability and ease of operation; (b) novel stimulator and recording circuit design, fully described; (c) possibility to evaluate different nerves, increasing the system usability; and (d) stimulation parameters digitally controlled with real-time feedback, through a user-friendly interface, which allows one to visualize the stimulus level before the stimulus application and brings safety while handling the equipment. Besides those benefits, the prototype was developed with readily available components; thus, the overall development cost of the device can be estimated at approximately \$ 150.00.

With regard to the NCS technique, some aspects must be carefully considered for the correct interpretation of the results and to reduce uncertainties. Physiological factors, including age and height and particularly temperature, can influence NCS responses [26]; lower temperatures tend to retard the propagation of the impulse while augmenting the amplitude of the nerve and muscle action potential [6]. Another factor that can cause error measurements is an inappropriate stimulus strength; supramaximal stimulation is required to ensure the activation of all nerve fibres [7]. One limitation of the NCS technique is finding the exact site of stimulation, as it is challenging to determine the nerve location from the surface.

Some limitations of this work are related to the NCS testing of only one nerve and lack of skin temperature monitoring. Follow-up studies should investigate the device validity in several nerves. Future versions of the device could incorporate a sensor to measure skin temperature, and also include a method, such as ultrasound, to identify nerves and guide recording and stimulating electrode placement [27]. Software improvement could include a protocol to define the supramaximal stimulus with an automatic peak detection algorithm, considering that the stimulus intensity is increased by 30% after the CMAP no longer increases [7].

## 5. Conclusion

A portable microcontroller-based electrostimulation system was proposed for nerve conduction studies, consisting of a stimulator, a recording system and a GUI. The system testing demonstrates that it can reliably deliver stimulus pulses and accurately record data. Also, the NCS parameters obtained from the cohort study were demonstrated to be within normal ranges established by the literature. The system has proven to be an integrated and functional solution and may be used as a POCD in the evaluation of neuromuscular functions (e.g., rapid and non-invasive screening test for diabetic peripheral neuropathy [13]).

## Acknowledgements

The authors thank the government funding agencies CAPES and CNPq for SC, FRA, MAF and ACA post-graduation scholarships. JLBm is a recipient of the productivity scholarship PQ-1D, supported by the National Council for Scientific and Technological Development (CNPq - Brazil).

## References

- [1] Mallik, A., Weir, A.I.: 'Nerve conduction studies: essentials and pitfalls in practice', *J. Neurol. Neurosurg. Psychiatry*, 2005, 76, (Suppl 2), pp. ii23–ii31
- [2] Webster, J.G.: 'Medical instrumentation: Application and design', (Wiley (USA), 2010)
- [3] Koo, Y.S., Cho, C.S., Kim, B.J.: 'Pitfalls in using electrophysiological studies to diagnose neuromuscular disorders', *J. Clin. Neurol.*, 2012, 8, (1), pp. 1–14
- [4] Dumitru, D., Nandedkar, S.D., Netherton, B.L.: 'Neurophysiology and Instrumentation'. AANEM 57th Annual Meeting, Québec, Canada, 2010
- [5] Kimura, J.: 'Nerve Conduction Studies', in Mills, K.R. (Ed.): 'Oxford Textbook of Clinical Neurology' (Oxford University Press, 2017, 1st edn.)
- [6] Kimura, J.: 'Electrodiagnosis in Diseases of Nerve and Muscle' (Oxford University Press, 2013, 4th edn.)
- [7] Daube, J.R., Rubin, D.I.: 'Nerve Conduction Studies', in Aminoff, M.J. (Ed.): 'Aminoff's Electrodiagnosis in Clinical Neurology' (Saunders, 2012, 6th edn.), pp. 289–325
- [8] Cadwell, J.A., Villarreal, R.A.: 'Electrophysiologic Equipment and Electrical Safety', in Aminoff, M.J. (Ed.): 'Aminoff's Electrodiagnosis in Clinical Neurology' (Saunders, 2012, 6th edn.), pp. 15–36
- [9] Buschbacher, R.M., Prahlow, N.D.: 'Manual of nerve conduction studies' (Demos Medical Publishing, 2006, 2nd edn.)
- [10] Preston, D., Shapiro, B.: 'Electromyography and Neuromuscular Disorders' (Elsevier, 2013, 3rd edn.)
- [11] Wang, A.K., Rutkove, S.B.: 'Electrophysiology of Polyneuropathy', in Blum, A.S., Rutkove, S.B. (Eds.): 'The Clinical Neurophysiology Primer' (Humana Press, 2007), pp. 275–288
- [12] Kong, X., Lesser, E.A., Gozani, S.N.: 'Nerve conduction studies: Clinical challenges and engineering solutions', *IEEE Eng. Med. Biol. Mag.*, 2010, 29, (2), pp. 26–36
- [13] Selvarajah, D., Kar, D., Khunti, K., et al.: 'Review Diabetic peripheral neuropathy: advances in diagnosis and strategies for screening and early intervention', *LANCET Diabetes Endocrinol.*, 2019, 8587, (19)

- [14] Lesser, E.A., Starr, J., Kong, X., Megerian, J.T., Gozani, S.N.: 'Point-of-Service Nerve Conduction Studies : An Example of Industry-Driven Disruptive Innovation in Health Care Point-of-Service Nerve Conduction Studies', *Perspectives in Biology and Medicine*, 2007, 50, (1), pp. 40–53
- [15] Scarr, D., Lovblom, L.E., Cardinez, N., et al.: 'Validity of a point-of-care nerve conduction device for polyneuropathy identification in older adults with diabetes: Results from the Canadian Study of Longevity in Type 1 Diabetes', *PLoS One*, 2018, 13:4
- [16] Himeno, T., Kondo, M., Sugiura-Roth, Y., et al.: 'Validity and reliability of a point-of-care nerve conduction device in diabetes patients', *J. Diabetes Investig.*, 2019, 10, (5), pp 1291-1298
- [17] Tolonen, U., Kallio, M., Ryhänen, J., et al.: 'A handheld nerve conduction measuring device in carpal tunnel syndrome', *Acta Neurol. Scand.*, 2007, 115, (6), pp. 390–397
- [18] Loi, D., Carboni, C., Angius, G., et al.: 'Peripheral neural activity recording and stimulation system', *IEEE Trans. Biomed. Circuits Syst.*, 2011, 5, (4), pp. 368–379
- [19] De Lima, J.A., Cordeiro, A.S.: 'A low-cost neurostimulator with accurate pulsed-current control', *IEEE Trans. Biomed. Eng.*, 2002, 49, (5), pp. 497–500
- [20] Sivaji, V., Grasse, D.W., Hays, S.A., et al.: 'ReStore: A wireless peripheral nerve stimulation system', *J. Neuroscience Methods*, 2019, 320, (October 2018), pp. 26–36
- [21] Stegeman, D.F., Van Putten, A.M.: 'Recording of neural signals, neural activation, and signal processing', in Mills, K.R. (Ed.): 'Oxford Textbook of Clinical Neurology' (Oxford University Press (UK), 2017), pp. 37–45
- [22] Ehler, E., Ridzoň, P., Urban, P., et al.: 'Ulnar nerve at the elbow - normative nerve conduction study.', *J. Brachial Plex. Peripher. Nerve Inj.*, 2013, 8:2
- [23] Benatar, M., Wu, J., Peng, L.: 'Reference data for commonly used sensory and motor nerve conduction studies', *Muscle Nerve*, 2009, 40, (5), pp. 772–794
- [24] Weitkamp, F., Elzenheimer, E., Schulte-Mattler, W., Schmidt, G., Laufs, H.: 'P15. Multimodal mapping of nerve pathology with a multichannel approach', *Clinical Neurophysiol.*, 2018, 129, (8), pp. e72–e73
- [25] Misra, U.K., Kalita, J.: 'An Introduction to Electrodiagnostic Signals and Their Measurements', in 'Clinical Neurophysiology' (Elsevier, 2006, 2nd edn.), pp. 11–20
- [26] Cossul, S., Favretto, M.A., Rettore Andreis, F., Marques, J.L.B.: 'Ulnar Motor Nerve Conduction Studies: Reference Values and Effect of Age, Gender and Anthropometric Factors', in Costa-Felix R., Machado J., Alvarenga A. (Eds.): 'XXVI Brazilian Congress on Biomedical Engineering' (IFMBE Proceedings, Springer, Singapore, 2019, 70/2)
- [27] Cartwright, M.S., White, D.L., Hollinger, J.S., Krzesniak-Swinarska, M., Caress, J.B., Walker, F.O.: 'Ultrasound guidance for sural nerve conduction studies', *Muscle and Nerve*, 2019, 59, (6), pp. 705–707

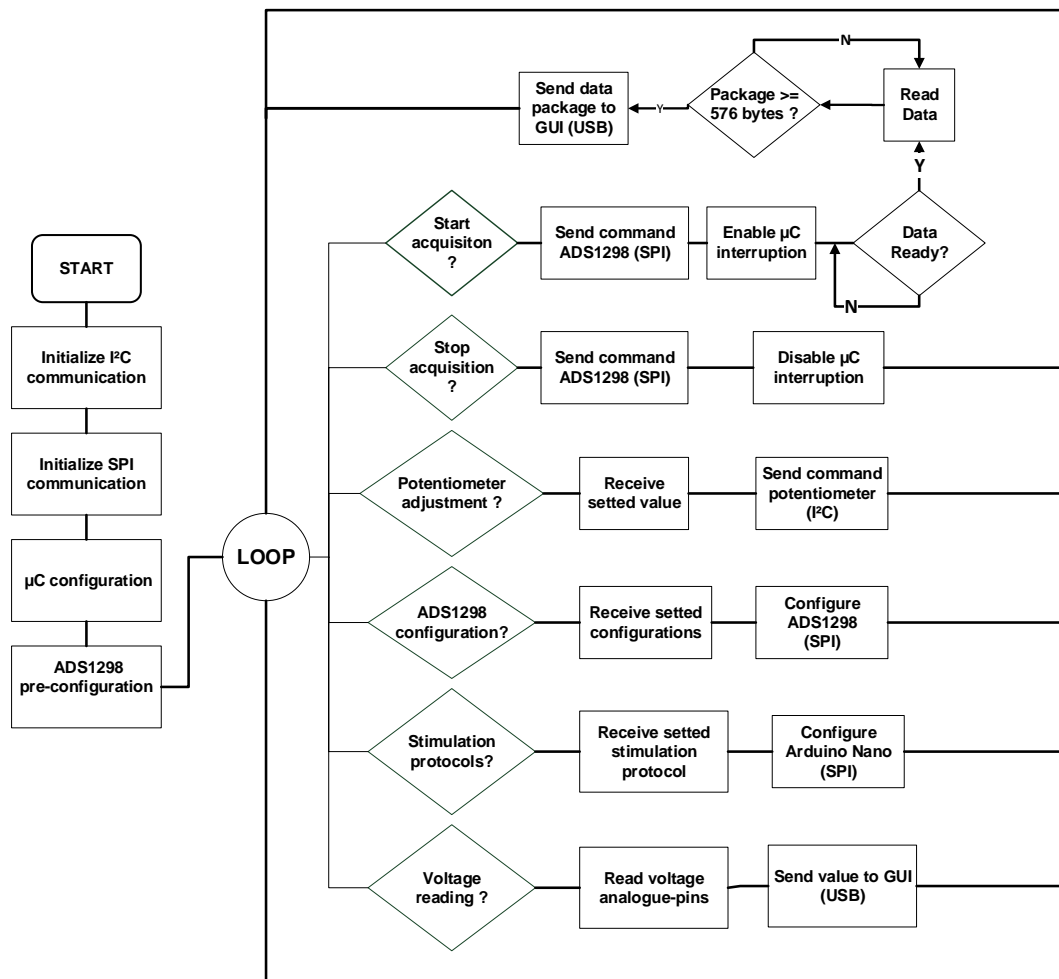


**Fig. 14** Implementation flowchart of the Teensy 3.2 microcontroller's (µC) firmware, as part of the controller module (CM). The functions of the µC include initialization of communication protocols (SPI and I²C), configuration of ADS1298 for data acquisition (voltage gain, data acquisition rate), configuration of the digital potentiometer according to the set value in the graphical user interface (GUI), configuration of the Arduino Nano µC, according to the selected stimulation protocol and reading of the analogue-to-digital (A/D) pins to measure the regulated voltage.